ACS EARTH AND SPACE CHEMISTRY

http://pubs.acs.org/journal/aesccq

Article

Brown Carbon Formation by Aqueous-Phase Reactions of Glycolaldehyde and Methylamine

Published as part of ACS Earth and Space Chemistry special issue "Hartmut Hermann Festschrift".

Camille L. Carthy, Erin O'Leary, Swetha Tadisina, Daniel R. Griffith, Heidi P. Hendrickson, Joseph L. Woo, and Melissa M. Galloway*

Cite This: https://doi.org/10.1021/acsearthspacechem.4c00200

Read Online

ACCESS | Metrics & More | Article Recommendations | Supporting Information

ABSTRACT: Brown carbon in aerosol remains a significant source of error in global climate modeling due to its complex nature and limited product characterization. Though significant efforts have been made to identify the major light-absorbing brown carbon chromophores formed through the reactions of small difunctional carbonyl-containing compounds with ammonium, substantial work is still required to identify the main absorbing species resulting from reactions of carbonyls with more complex amines. Using tandem mass spectrometry and isotopic substitution experiments to confirm proposed structures and support their mechanistic pathways, evidence is provided for the formation of N-containing oligomers and heterocycles in glycolaldehyde + methylamine reaction systems. Decomposed time-resolved UV–visible absorbance spectra infer multiple parallel reactions occurring at different rates. Surface tension measurements identify potential amphiphilicity in reaction products. Theoretical time-dependent density-functional theory calculations provide insight into the light absorption properties of individual molecules within the complex reaction mixture. These products may contribute to brown carbon light absorption, thus holding significant relevance toward accurately predicting their effects on global climate.

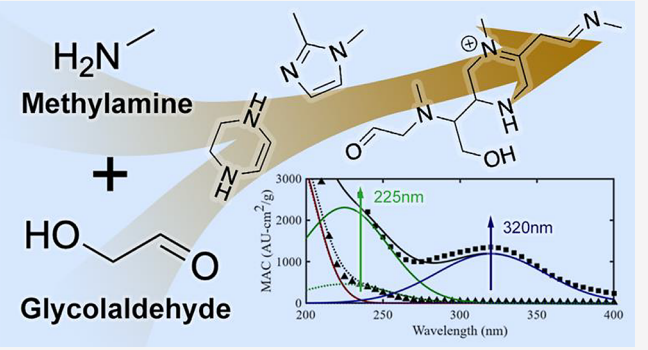

KEYWORDS: *glycolaldehyde, methylamine, density functional theory, brown carbon, SOA, atmospheric chemistry*

INTRODUCTION

The complex nature of the light absorbance properties of brown carbon (BrC) compounds highlights the importance of determining their composition and contribution to climate modeling. Aqueous aerosols containing small water-soluble carbonyls react with ammonium salts and amines to produce BrC, which absorb light in the near-ultraviolet and visible regions.[1,2] In addition to their climate effects, BrC are part of the fine fraction of particulate matter ($PM_{2.5}$) and are small enough to cross the blood brain barrier, traveling from the respiratory to the central nervous system (CNS).[3] This disruption of the blood brain barrier poses a risk to human health.[3] Furthermore, BrC compound formation reactions are typically irreversible,[4] leading to more persistent particles in the atmosphere, and thus increasing $PM_{2.5}$ exposure and amplifying the health risks observed from air pollutant exposure. The physical characteristics of the particle itself also determine the pathophysiological alterations in the CNS that result from inhaling particulate matter, emphasizing the importance of identifying the atmospheric constituents of $PM_{2.5}$.[3]

Glycolaldehyde (GAld) and other notable carbonyl-containing volatile organic compounds (CVOCs) are abundant in the atmosphere and originate via gas phase oxidation of biogenic (e.g., isoprene) and anthropogenic emissions of volatile organic compounds.[5−9] Global production of GAld from isoprene oxidation via the OH radical has been estimated to be 42 Tg C $year^{-1}$,[10] with cloud droplet concentrations of 0.3−3.6 μM and aerosol concentrations of 0−1300 pmol m^{-3}.[1] Methylamine (MeAm) emission is linked to various sources but most predominantly to biomass burning, animal husbandry and oceanic activities.[11] Ambient MeAm concentrations have been observed to be 0.03−0.06 μM (cloudwater) and 56 ± 52 pmol m^{-3} (aerosol droplets).[1] The abundance and reactivity of GAld and MeAm in the atmosphere emphasize the need for

Received: July 5, 2024
Revised: August 7, 2024
Accepted: August 9, 2024

further investigation to incorporate this system in atmospheric models.[11−13]

Critical research on the reactions between glyoxal (Gly), GAld, methylglyoxal (MGly), and hydroxyacetone (HA) with ammonium sulfate (AS) and amines have revealed the capacity for these carbonyl-containing and nitrogen-containing compounds to form heterocyclic products, including furan, imidazole, and pyrazine derivatives.[1,5,6,14−18] However, the reactions between GAld and MeAm have been seldom studied,[1,19,20] and thus much uncertainty remains regarding the product formation and brown carbon importance of this system.

Powelson et al. studied the reaction of GAld with AS and determined that aldol condensation is not likely to be a significant reaction pathway,[1] while Yi et al. proposed several open chain oligomers and oxazine-derivatives.[19] Grace et al. shed new light on the likelihood of GAld + AS to undergo aldol condensation reactions in which AS nucleophilically attacks the carbonyl carbon, and is therefore the first to propose the formation of aromatic heterocycles in the system.[15] Rodriguez et al. observed similar long chain and oligomers in aqueous GAld + AS particles, including an imidazole derivative, consistent with the findings of Grace et al.[15,20] The reactivity of MeAm with carbonyls was explored by De Haan et al.[13,17,21−23] and Yi et al.[12,19] De Haan et al. proposed a mechanism of imine formation followed by rapid dimerization and oligomer formation for the Gly + MeAm reaction system.[13] Yi et al. additionally studied the reaction kinetics and product formation from reactions of HA and MeAm.[12] Like GAld, HA is a water-soluble carbonyl produced by the oxidation of isoprene. Yi et al. proposed a mechanism of aldol condensation by which HA undergoes nucleophilic attack by MeAm to produce imine-dominated brown carbon.[12] The reactions of HA and MeAm are estimated to account for 1% of the light absorption of atmospheric brown carbon.[1,12] Given that HA is slightly less abundant than GAld in the atmosphere,[1] this estimation highlights the impact of seemingly low concentrations of carbonyls on BrC and furthers the need to investigate the GAld + MeAm system.

Together, these studies support the interaction between GAld and MeAm and provide insight into mechanistic pathways. Yi et al. proposed a reaction scheme for the GAld and MeAm system but notably, only proposed one aromatic compound (1,3-methylimidazole) and do not suggest a mechanism for formation.[19] De Haan et al. showed that the reaction of MGly + MeAm will form aromatic compounds, supporting the idea that aromatic compound formation from carbonyl + MeAm systems is possible.[17,23] Rodriguez et al. found that the exposure of MeAm to GAld + AS seed aerosol resulted in further imidazole product formation.[20] Given all of this, further work is necessary to more comprehensively characterize this reaction system.

As several other CVOC aqueous secondary organic aerosol (SOA) reaction systems have demonstrated marked effects on the overall physical properties of the solutions in which they are contained, it is likely that the analogous chemistry that occurs in the GAld + MeAm system will also yield products that exhibit UV-absorptive or surfactant effects. The methyl group on BrC precursors such as MGly may lead to increased surfactant or chromophoric properties in the reaction mixtures as compared to Gly systems.[24−26] While GAld does not have this same methyl group, the MeAm may be able to provide a similar degree of methylation in the product mixture. Powelson et al. showed that the light absorption of the GAld + MeAm system is significantly larger than the GAld + AS system.[1] Yi et al. used UV−visible spectroscopy to determine that light absorption reaction kinetics of the GAld + MeAm system are in the range of $1.2-3.5 \times 10^{-6}$ s^{-1}, and are somewhat dependent on MeAm concentration (0.5−2.5 M MeAm and 0.1 M GAld).[19] When compared to the GAld + AS reaction rates they calculated ($8.33 \times 10^{-7}-1.39 \times 10^{-6}$ s^{-1}), this indicates that the MeAm system may have slightly faster reaction kinetics than the AS system. To the authors' knowledge, no surface tension studies have been performed on the GAld + MeAm system.

Computational studies on the light absorption of BrC mixtures have helped to elucidate the compounds responsible for the BrC character of the total solutions.[14,15,17] Grace et al. determined that increasing conjugation of aromatic compounds leads to light absorption that tails into the visible region, which is a characteristic of BrC.[15] However, they also found that a single methylation can provide a slight redshift in light absorption and increase in molar absorptivity, due to the slight increase in electron delocalization in the methylated molecule.[15] Compared to AS, MeAm products tend to be more methylated in general, so this could lead to systems with higher absorptivity in the visible region.

This work is consistent with previous studies on carbonyl and amine reactions, supporting the formation of imine and N-containing oligomers through a series of aldol condensation, imine dimerization, and dehydration reactions.[17,19,23] We further propose the first mechanism for the formation of aromatic imidazole derivatives in the GAld + MeAm reaction system, which are corroborated via supercritical fluid chromatography−tandem mass spectrometry and ^{15}N isotopic substitution experiments. Density functional theory calculations, UV−visible spectroscopy reaction kinetics, and surface tension measurements further support these identifications.

MATERIALS AND METHODS

Reagents. Aqueous methylamine (40 w/w% in H_2O) and solid glycolaldehyde dimer were purchased from Sigma-Aldrich. For the isotopic substitution experiments, ^{15}N-MeAm:HCl (98%) was purchased from Cambridge Isotope Laboratories, Inc. Food grade carbon dioxide was obtained from Airgas, while methanol (Optima LC/MS grade), formic acid (Optima LC/MS grade), and sodium hydroxide (0.1 N standard solution) were purchased from Fisher Chemical.

Preparation of GAld + MeAm Standards. Separate standard solutions of 1 M each of GAld, MeAm, and ^{15}N-MeAm: HCl were prepared by dissolving each compound in Millipore Milli-Q Ultrapure water (18.2 MΩ cm resistivity). All standard solutions were used within one month of preparation.

SFC-MS/MS. Solutions analyzed using supercritical fluid chromatography−tandem mass spectrometry (SFC-MS/MS) contained 50 mM GAld + 50 mM MeAm and were aged for 24 h under dark conditions at room temperature. Analogous sets of 50 mM GAld + 50 mM ^{15}N-MeAm:HCl + 50 mM NaOH were prepared for the isotopic substitution experiments. Equimolar NaOH was included in the reaction mixture for ^{15}N experiments to neutralize the HCl. Samples were analyzed using a Waters ACQUITY Ultra Performance Chromatography (UPC^2) supercritical fluid chromatography system coupled to a Waters XEVO TQD tandem quadrupole mass spectrometer. This technique is described in detail by Grace et

https://doi.org/10.1021/acsearthspacechem.4c00200
ACS Earth Space Chem. XXXX, XXX, XXX−XXX

al.[27] A binary gradient of CO_2 and methanol was used for elution of all samples through a Viridis UPC^2 BEH column (2.1 × 100 mm, 1.7 μm particles). Starting conditions of 98% CO_2 and 2% methanol were held for 2 min. Then the modifier content was increased to 20% until 18 min before the system returned to initial conditions at 18.5 min and held for 1.5 min. The total flow rate was held constant at 1.0 mL/min with 0.50 mL/min MeOH + 10 mM formic acid makeup flow. The UPC^2 system back pressure was set to 1500 psi for the duration of all sample runs. Positive mode ESI conditions were set as follows: capillary voltage = 1.18 kV, cone voltage = 30 V, desolvation temperature = 250 °C, desolvation gas flow = 650 L/h, and cone flow = 1 L/h. Once a mass was identified in the mass spectrum, the sample was reanalyzed using selected ion monitoring (SIM) to provide better sensitivity. Tandem mass spectrometry (fragmentation voltage = 20 eV) was also utilized to determine structural features.

Kinetics Experiments. A Cary 3500 Compact Peltier UV−visible spectrometer was used to measure the absorbance of aqueous GAld + MeAm samples blanked against a background of Milli-Q water. A constant volume of 400 μL of solution was added to a 1 mm path length quartz cuvette (Starna Cells) and five sets of reaction conditions were tested: 5, 50, and 500 mM GAld were individually reacted with 50 mM MeAm while 5, 50, and 500 mM MeAm were individually reacted with 50 mM GAld. These concentrations were chosen to test reaction kinetics across a range of atmospheric conditions. To analyze the lower absorbance regions, a constant volume of 4000 μL of solution was added to a 1 cm path length quartz cuvette (Starna cells) and the following four sets of reaction conditions were tested: 50 and 500 mM GAld were individually reacted with 50 and 500 mM MeAm. The absorbance of each solution was collected over the range of 190−600 nm every 2 min for 48 h in a temperature-controlled cuvette holder maintained at 18 °C. The observed mass losses for the GAld + MeAm solutions were comparable to the blank.

These time-resolved absorbance spectra were decomposed into multiple peaks using MATLAB (Mathworks, 2022b), consistent with the methods applied in Fan et al.[28] and Grace et al.[14] Briefly, absorbance, A, is fitted assuming that three combined Gaussian lineshapes with constant location, c_i, and spread, σ_i, can represent its wavelength dependence:

$$\mathrm{MAC}(\lambda, t) \approx \sum_{i}^{3} \left[M_{c,i} + M_i \left(1 - \exp\left(-\frac{t}{M^I_{\tau,i}} \right) \right) \right] \cdot \exp\left(-\left(\frac{\lambda - c_i}{\sigma_i} \right)^2 \right) \quad (1)$$

The temporal dependence of each component peak was expressed assuming first-order kinetics, resulting in an initial absorbance value $M_{c,i}$ rising with exponential decay by an offset value of M_i with a time constant of $M^I_{\tau,i}$. From the initial loading of MeAm in the solution mimic, $[\mathrm{MeAm}]_0$, an estimation of rate of formation can be obtained through $M^I_{\tau,i}$:

$$k^I = \frac{1}{[\mathrm{MeAm}]_0 M^I_{\tau,i}} \quad (2)$$

This approach enables the deconvolution of multiple overlaid absorbance peaks in a given spectra to two or more potential chromophoric pathways. While not representative of the light-absorbing properties of any one specific compound, it is assumed that similarly structured SOA products will exhibit similar formation kinetics and absorbance properties to one another. The inferred rate constants can therefore be treated as proxies for different families of SOA chemistry or combined multiple-step reactions that result in products that concurrently form in the GAld + MeAm reaction system. As in similar works that use this method of kinetic fitting,[5,14,28] the inferred rate constants assume a roughly constant concentration of nitrogen-containing reactant, which will result in upper-bound estimations for chemical kinetics where potential depletion effects may occur over the duration of the modeled period. While depletion of the methylamine is possible within these systems, the overall concentrations of the chromophoric products are far less than that of the GAld or MeAm, which would result in low to negligible depletion effects of the chromophores in solution.

The absorbance efficiency of these aerosol mimic solutions can be expressed in terms of a mass absorbance coefficient, $\mathrm{MAC}(\lambda)$, which is scaled from the measured absorbances, $A(\lambda)$, by the total initial organic loading and the path length of measured absorbance, l:

$$\mathrm{MAC}(\lambda) = \frac{A(\lambda)\cdot \ln 10}{l \cdot \sum_i c^{\circ}_{\mathrm{org},i} \cdot \mathrm{MW}_{\mathrm{org},i}} \quad (3)$$

Here, the individual initial molar concentrations $c^{\circ}_{\mathrm{org},i}$ of each organic compound (i.e., MeAm and GAld) are multiplied by their molecular masses $\mathrm{MW}_{\mathrm{org},i}$ and summed.

Surface Tension Measurement. Surface tension measurements were obtained from aqueous aerosol mimic solutions containing 500 mM GAld + 500 mM MeAm. Solutions were aged for 24 h under dark conditions at room temperature. The surface tension of 10 μL droplets was measured via pendant drop tensiometry at 2 s intervals in a modified profile analysis tensiometer (SINTERFACE, Inc.), as described in Beier et al.[24] Droplets were suspended in ambient conditions from a 0.9 mm-diameter, blunt-tip needle for 3 min during data collection, to allow for solution equilibration.

Computational Methods. Calculations were carried out following the procedure presented in previous studies.[14,15] Density functional theory (DFT) calculations were conducted using the Gaussian 16 software package.[29] The ωB97X-D[30,31]/6-311G(2d,p)[32,33] level of theory was used for all compounds. The conductor-like polarizable continuum model (CPCM) was employed to account for the solvent environment, with water as the solvent.[34,35] Ground state geometries for each compound were optimized and frequency calculations were performed to confirm the stability of the calculated energy minima on the potential energy surface.

Time-dependent Density Functional Theory (TDDFT) was used to compute the 15 lowest-energy excitations for each compound. Based on previous work,[14,15] a red shift of −0.6 eV was applied to calculated excitation energies to provide a quantitative agreement between calculated and experimentally observed spectra. Both red-shifted and nonred-shifted excitation energies and corresponding oscillator strengths are provided in Table S2. Natural Transition Orbitals (NTOs)[36] were visualized using iQmol v2.14.0.[37]

The construction of a simulated absorption spectrum requires applying a Gaussian broadening function to each computed excitation to account for inhomogeneous line-

https://doi.org/10.1021/acsearthspacechem.4c00200
ACS Earth Space Chem. XXXX, XXX, XXX−XXX

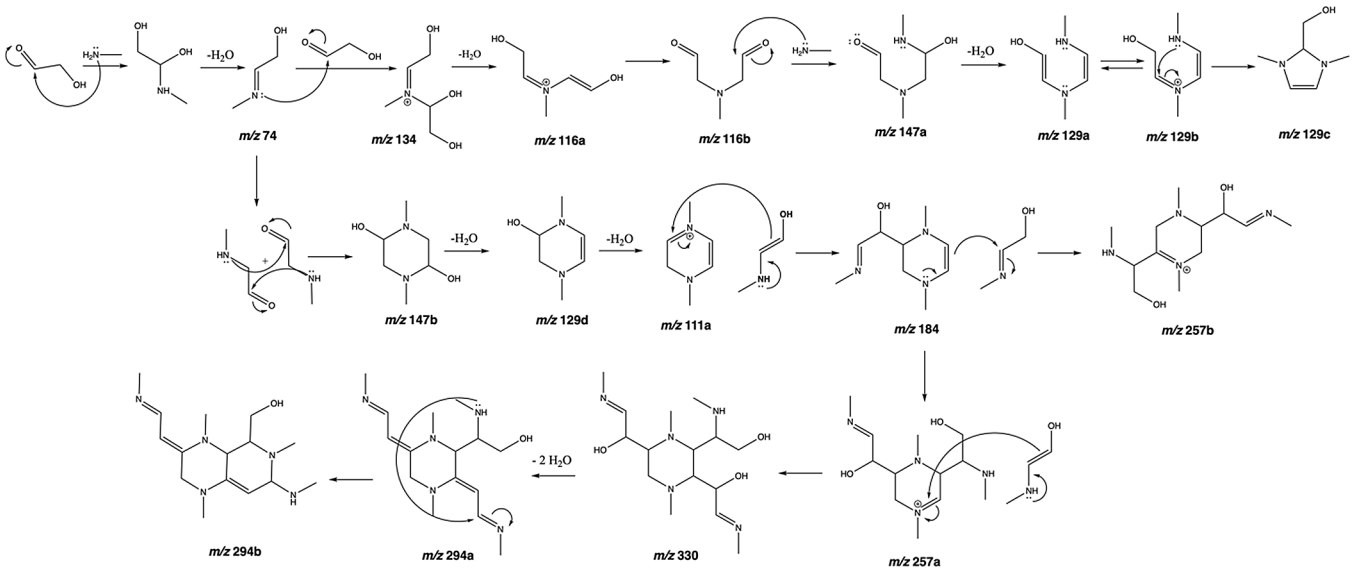

Figure 1. Proposed mechanism for formation of N-containing oligomers, heterocyclic, and polycyclic compounds.

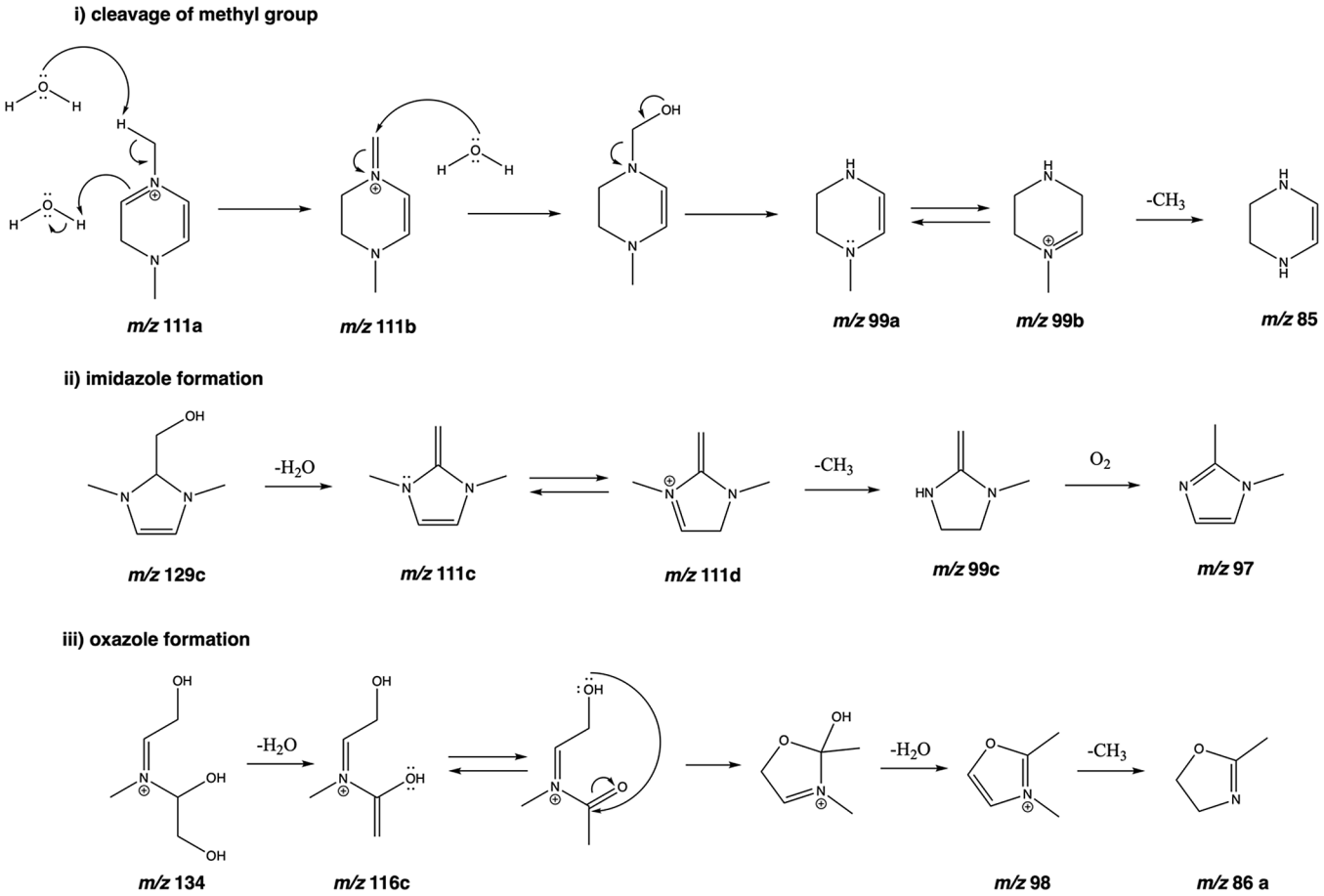

Figure 2. Proposed mechanism for (i) the cleavage of CH_3 groups, leading to formation of (ii) imidazole and (iii) oxazole derivatives in the GAld + MeAm system.

broadening. The broadening function was applied based on the protocol in GaussView 6 according to[38]

$$\varepsilon_i(\tilde{\nu}) = \frac{\sqrt{\pi}\cdot e^2\cdot N}{1000\cdot \ln(10)\cdot c^2\cdot m_e}\frac{f_1}{\sigma}\exp\left[-\left(\frac{\tilde{\nu}-\tilde{\nu}_i}{\sigma}\right)^2\right] \quad (4)$$

where $\varepsilon_i(\tilde{\nu})$ is the extinction coefficient for excitation, i, e is the fundamental unit of charge, c is the speed of light, N is Avogadro's number, and m_e is electron mass. The values f_i and $\tilde{\nu}_i$ refer to energy (in wavenumbers) and oscillator strength, respectively, for each excitation, i. The standard deviation of the Gaussian curve, σ, in wavenumbers, was set to the default

https://doi.org/10.1021/acsearthspacechem.4c00200
ACS Earth Space Chem. XXXX, XXX, XXX−XXX

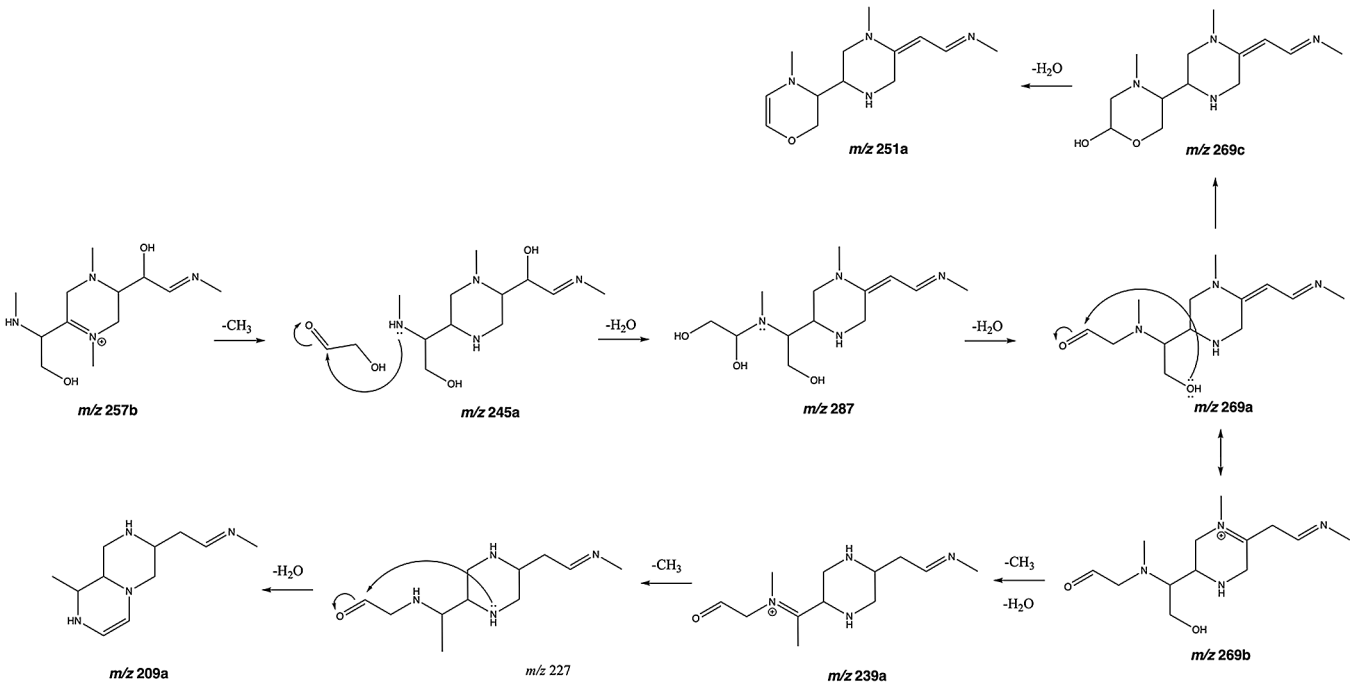

Figure 3. Proposed mechanism for formation of heterocyclic and polycyclic compounds following demethylation of the nitrogens.

value in GaussView 6, which is σ = 0.4 eV. The overall spectrum, $\varepsilon(\tilde{\nu})$, was generated by summing the contributions of each excitation to the overall spectrum for each molecule according to

$$\varepsilon(\tilde{\nu}) = \sum_{i=1}^{n} \varepsilon_i(\tilde{\nu}) \tag{5}$$

RESULTS AND DISCUSSION

Product Characterization. The observed product masses and formation of GAld dimers and trimers are consistent with the results of Yi et al.[19] and Kua et al.[39] The formation mechanisms for pyrazine, piperazine, imidazole, and oxazole derivatives as well as other heterocycles and N-containing oligomers are also proposed herein. All proposed structures can be found in Table S1. All structures are supported by ^{15}N-MeAm experiments to corroborate the proposed number of nitrogens within each molecule and tandem mass spectrometry experiments to determine common structural features and fragment losses.

GAld reacts with MeAm to produce an imine (m/z 74). The imine condenses with additional molecules of GAld and MeAm to form N-containing oligomers, undergoing dehydration reactions in the process (Figure 1). The dehydration product of oligomer m/z 147a can cyclize to form a potential imidazole precursor (m/z 129c). Alternatively, imine dimerization leads to 2,5-dihydroxypiperazine (m/z 147b), which subsequently dehydrates to form unsaturated derivatives (m/z 129d, 111a). Iminium and enamine tautomers may further react with m/z 111a to produce larger pyrazine derivatives (m/z 184, 257a, 257b). Nucleophilic addition of an additional GAld-derived enamine to m/z 257a forms the neutral piperazine derivative m/z 330. Subsequent dehydration of m/z 330 results in monocyclic and bicyclic isomers m/z 294 (Figures 1 and S2).

Compared to previously studied carbonyl-ammonium reaction systems,[6,15,16] the nitrogens in the GAld + MeAm system are methylated. This study is the first to propose a mechanism to cleave the N−CH_3 bond in the GAld + MeAm system via isomerization and hydrolysis of the iminium ion. Formaldehyde is formed as a byproduct in the process. Figure 2i illustrates the intermediates involved in the first demethylation of m/z 111a to produce m/z 99a. Further demethylation is annotated as −CH_3. Through the same demethylation mechanism, m/z 129c forms m/z 99c. Oxidation of m/z 99c produces 1,2-dimethylimidazole (m/z 97), the first stable aromatic compound to be reported in the GAld + MeAm system (Figure 2ii). An oxazole derivative (m/z 86) is also formed as a result of demethylation: dehydration of m/z 134 results in m/z 116c, which cyclizes to form 1,2-dimethyl oxazolium ion, m/z 98, and then undergoes demethylation to form 2,3-dihydro-2-methyloxazole (m/z 86, Figure 2iii).

Following an analogous mechanism to that shown in Figure 1, m/z 257b can be demethylated at both the 1 and 4 positions to produce heterocyclic and polycyclic compounds (Figure 3). The cleavage of the first methyl group produces m/z 245a, which then condenses with GAld. Subsequent dehydration results in m/z 287 and m/z 269a, which cyclizes to m/z 269c (Figure 3). The two peaks in the EIC for m/z 269 likely correspond to the monocyclic and polycyclic isomers (Figures 3 and S1). Alternatively, the iminium form (m/z 269b) enables the cleavage of the second methyl group from the ring and after dehydration, produces m/z 239a. Demethylation and dehydration of m/z 239a results in bicyclic compound m/z 209a (Figure 3).

Overall, the GAld + MeAm system appears to yield fewer aromatic products than the GAld + AS and similar CVOC + AS systems.[15,16,40] However, saturated analogs of such aromatic compounds are formed. These tend to be highly conjugated due to the high degree of GAld oligomerization. Nitrogen demethylation is also possible with many of these

https://doi.org/10.1021/acsearthspacechem.4c00200
ACS Earth Space Chem. XXXX, XXX, XXX−XXX

compounds, leading to a number of the corresponding demethylated analogs.

Light Absorbance. All GAld + MeAm solutions demonstrated high absorption in the near-UV and tailing into the visible region (black points, Figure 4), similar to other

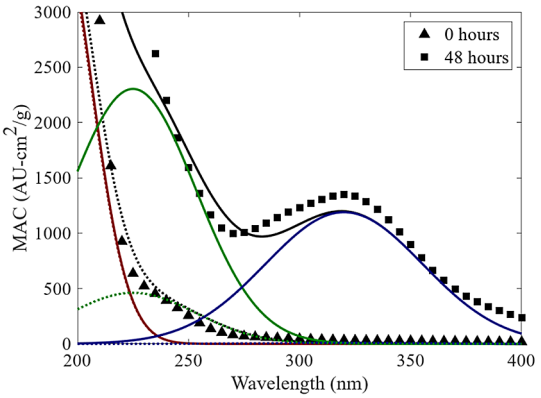

Figure 4. Observed UV−visible spectra for the 50 mM GAld + 50 mM MeAm system (points) and approximated absorbance values using a three-curve Gaussian decomposition for 0 (dotted) and 48 h (solid) of solution aging.

carbonyl + ammonium/amine systems in broad shape but exhibiting a nearly 10-fold higher MAC compared to the GAld + AS reaction system.[1,15,19,28] Higher MAC values were observed for higher MeAm loading, though rate constants inferred through these absorbance readings did not show any meaningful trends with respect to MeAm once concentration was accounted for (eq 3).

Density functional theory calculations were performed for each identified product. A subset of calculated absorption spectra that have excitations within the 290−350 nm range can be found in Figure 5, while calculated absorption spectra for all identified structures can be found in Figures S9−S13. Specific excitation energies and oscillator strengths for the 15 lowest-lying excitations of each individual compound are also provided in Table S2. Calculated absorption wavelengths for structures identified in the GAld + MeAm reaction fall within the 150−450 nm range, similar to the absorption ranges identified in previous work.[14,15] In the compounds identified here, the lowest lying excitations can mostly be described by either $\pi-\pi^*$ transitions or $n-\pi^*$ transitions involving e.g., the nonbonding lone pair electrons on the nitrogen atoms.

Experimentally measured absorbances of solutions over 48 h were decomposed into three modeled absorption peaks, each with differing location, magnitude, and rate of growth (solid lines, Figure 4). The largest of these peaks, occurring at approximately 200 nm, did not exhibit meaningful kinetics (k^I < 0.001 $h^{-1}\cdot M^{-1}$). Absorbance in this region can be attributed to a combination of nonreactive, smaller functional groups or CVOC oligomeric products, including imidazoles (previously at ∼195 nm),[5] α-dicarbonyl groups (previously attributed to ∼208 nm in similar reaction systems),[28,41] and MeAm itself, which absorbs strongly in <200 nm regions. The majority of the compounds identified in this work also contribute to absorption in this region (Figures S9−S13 and Table S2), supporting previous research indicating that this peak cannot be used to help determine functional groups present in the mixture, but instead gives an overall view of reaction progress.[14]

A second decomposed peak, located at approximately 225 nm, overlapped with the 200 nm peak but steadily grew in magnitude over the entire duration of absorbance measurement (k^I = 0.375 $h^{-1}\cdot M^{-1}$). Fan et al. observed a similar overlapping peak at 213 nm for aged GAld + AS bulk mixtures with comparable kinetics (k^I = 0.297 $h^{-1}\cdot M^{-1}$),[28] with absorbance in this region being attributed to imidazole derivatives across multiple previously reported works,[15,42] suggesting analogous chemistry in this work with slight red-shifting due to the increased methylation of MeAm. Many of the conjugated, nitrogen-containing compounds identified in this work contribute to this absorption peak (e.g., m/z 111, 158, 239, 294; Figures S9−S13 and Table S2).

A third, wider peak, located at approximately 315−320 nm, exhibited negligible contribution to solution absorbance at

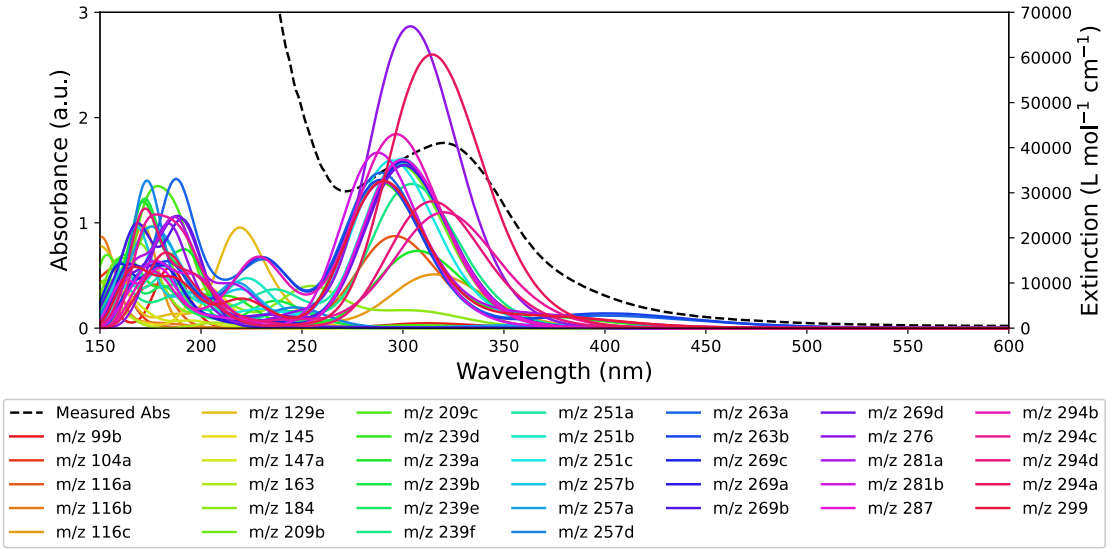

Figure 5. Observed UV−visible spectra for the 50 mM GAld +50 mM MeAm system after 48 h of aging (dashed black, left y-axis); calculated absorption spectra for a subset of compounds identified herein (solid colors, right y-axis). The extinction coefficient was calculated according to eq 5.

https://doi.org/10.1021/acsearthspacechem.4c00200
ACS Earth Space Chem. XXXX, XXX, XXX−XXX

short aging times but was observed to slowly evolve over the recorded 48 h period (k^I = 0.024 $h^{-1}{\cdot}M^{-1}$). This peak does not appear in the GAld + AS system, which instead has demonstrated a peak at 269 nm that was previously attributed to pyrazine derivatives.[15] This being said, MGly + ammonium reaction systems have demonstrated small contributing absorbance peaks at 340 nm, consistent with MGly aldol condensation products.[28] The longwave UV absorbance of this peak is also similar to other lesser-contributing, nitrogen-containing chromophoric species observed by Lin et al. in MGly-ammonium reaction systems, though inconsistencies between m/z values noted in Lin et al. and those seen here imply that the specific light-absorbing compounds that are formed are not the same despite similar molecular weight, oxygenation, and nitrogenation.[16] The GAld + MeAm system is less likely to form the highly substituted imidazole and pyrazine compounds often found in α-dicarbonyl (i.e., Gly, MGly, and biacetyl) + ammonium/amine reaction mixtures,[14,16,18] making it likely that the chromophoric nature of this system arises from different classes of compounds. Most of the reaction products identified in this study that contribute to this peak have m/z > 200, contain multiple nitrogens, and are more conjugated than the compounds that contribute to the 225 nm peak. Specifically, the strongly absorbing excitations in this region can be attributed to the vinylogous amidine groups in these compounds, where the π-conjugation extends from the imine group to the lone pair of the adjacent tertiary amine. The effect of the vinylogous amidines is illustrated by the comparison of example compounds provided in Figure 6A,B. The highest occupied transition orbitals (HOTO) and lowest unoccupied transition orbitals (LUTO) represent the electronic excitation as a single electron transition between HOTO and LUTO and are also shown for relevant excitations in Figure 6. The imine in m/z 209c (Figure 6A) is not conjugated to the iminium ion, and thus the lowest-lying excitation is a n−π* transition involving the nitrogen lone pairs. However, in m/z 209b (Figure 6B), the conjugation extends from the imine to the tertiary amine, which results in the lower-lying π−π* excitation that contributes to the 320 nm peak.

Therefore, this peak is likely to be a result of larger compounds that are formed due to extensive oligomerization of the GAld and MeAm. The species that absorb most strongly in this region are heterocyclic. In addition, modeled kinetics for this third peak in the 320 nm region consistently overestimated absorbance in short- to intermediate (~12−24 h) aging but underestimated over longer periods, implying that first order kinetics may not be sufficient to fully encapsulate the chemical phenomena taking place. These compounds require multiple oligomerization steps to form and will only begin to form once intermediate precursors further react, delaying their formation and therefore, light absorption.

A small subset of molecules (e.g., m/z 111a, 111b, 111d, 129b) exhibit calculated absorptions above 390 nm. While the experimental absorption spectra do not contain a distinct absorption peak in this region, these molecules may contribute to a small shoulder on the peak near 320 nm. These compounds are all conjugated iminium cations with two nitrogen atoms (hydropyrazines, hydroimidazoles, and long chain nitrogen-containing oligomers). As illustrated in Figure 6C,D, the excitations in this region involve the iminium cation. For example, m/z 251b (Figure 6C) and m/z 263b (Figure 6D) differ by an iminium ion in m/z 263b that is not present in m/z 251b. The π−π* transitions in m/z 251b and m/z 263b

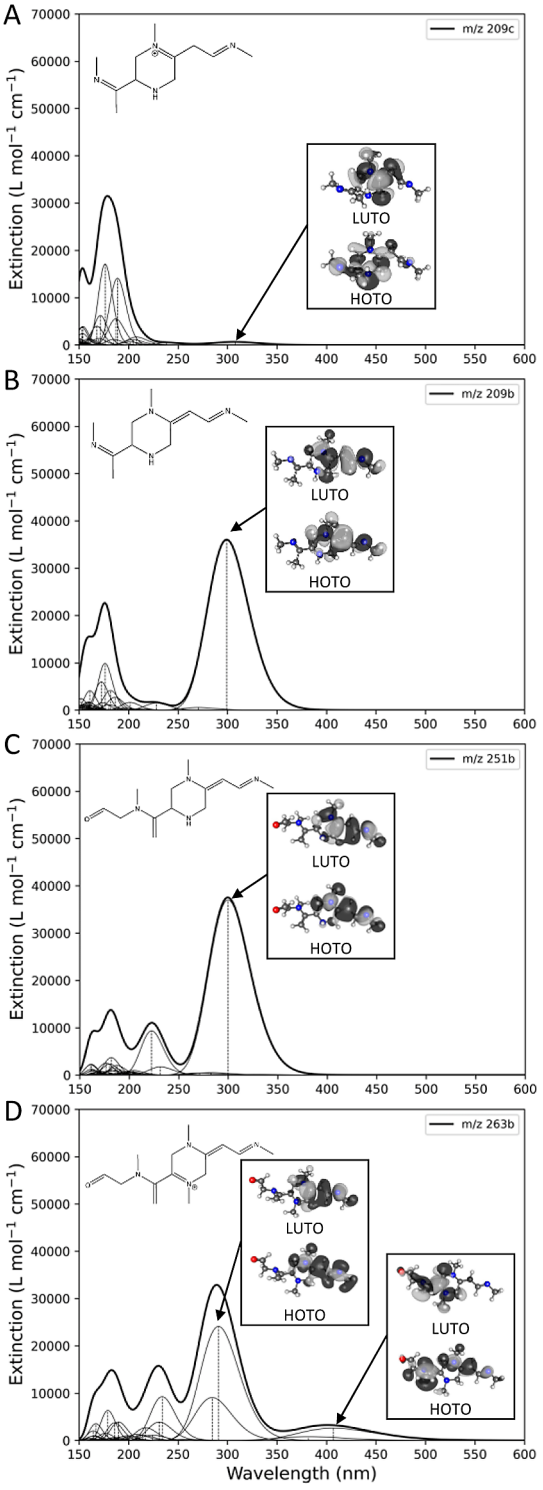

Figure 6. Calculated UV−visible absorption spectra of compounds (A) m/z 209c, (B) m/z 209b, (C) m/z 251b, and (D) m/z 263b. The highest occupied transition orbitals (HOTO) and lowest unoccupied transition orbitals (LUTO) are shown for select transitions indicated by the black arrows.

have significant relative extinction coefficients. The low-lying excitations in m/z 263b (Figure 6D) involving the iminium ion are not present in m/z 251b. These excitations have a smaller absorption intensity due to the charge transfer nature of the excitations, where the electron density shifts to the cation upon excitation, as shown in Figure 6D.

https://doi.org/10.1021/acsearthspacechem.4c00200
ACS Earth Space Chem. XXXX, XXX, XXX−XXX

Surface Tension. Surface tension of 500 mM MeAm/500 mM GAld solutions were measured to be 67.6 ± 1.0 dyn/cm. These mixtures demonstrated similarity to 500 mM MeAm solutions (68.7 ± 0.4 dyn/cm), though 500 mM GAld solutions exhibited significantly lower surface tension (59.8 ± 0.2 dyn/cm) compared to either MeAm or GAld/MeAm mimic solutions. Further, mixture aerosol mimics between 0 and 24 h did not show a statistically significant difference in surface tension as a function of solution age (p = 0.737).

Shifts in surface activity in aqueous SOA can imply changes to the relative moieties of the compounds that compose them; products that are more amphiphilic in nature will lead to surface tension depression. These products are likely to contain nonpolar and polar regions in their overall structure, which imparts additional insight into candidate structures. Conversely, a lack of surface tension depression would imply that the products formed do not contain sufficient amphiphilicity or asymmetry to shift the overall physical properties of the total solution. Since no change in surface tension was observed over the 24 h reaction period and there is little difference in surface tension between MeAm and the aged GAld + MeAm solutions, it is proposed that the reaction products in the GAld + MeAm mixture do not contain the same amphiphilic nature as the MGly + AS products. This may be a result of the demethylation reactions described above that have not been observed in the MGly + AS system, but it is more likely to be a result of the placement of methyl groups on the products resulting from MeAm reactions. A methyl group that is linked to the rest of the molecule via a carbon−nitrogen bond (as is often the case in the GAld + MeAm products) will be more polar than a methyl group attached via a carbon−carbon bond (as observed in MGly + AS products). Therefore, the surface activity of these molecules will be different even if the overall shape and structure of the molecule is similar (e.g., 1-methylimidazole vs 4-methylimidazole). The lack of surface activity of the product molecules observed in the GAld + MeAm system indicates that the degree of methylation of a system is not the only factor that should be used in determining its surface activity.

Atmospheric Implications. The results presented in this work demonstrate a logical extension of the broad findings and trends observed in other CVOC-containing reaction systems. The nitrogen-based chemistry occurring between GAld and MeAm results in products analogous to those observed between GAld and AS, though with enhanced chromophoric behavior that is more in alignment with MGly-ammonium chemistry. The reaction products formed in the GAld + MeAm reaction system do exhibit some differences to those found in CVOC + ammonia/amine reaction systems. At lower product masses (e.g., dimers), imidazoles and oxazoles are formed in many of these reaction systems,[15] and were observed in the GAld + MeAm system as well. However, as an α-hydroxycarbonyl reacting with a primary amine, the ring formation step to create imidazoles, pyrazines, and oxazoles is not as favorable compared to α-dicarbonyls (e.g., Gly, MGly, etc.) This being said, the GAld/MeAm system forms other heterocyclic and open-chain compounds such as piperazines, hydropyrazines, hydroimidazoles, and hydrooxazoles, along with many iminium cations. Many of these products are more methylated in nature than the GAld + AS reaction system because of the MeAm precursor, which leads to an overall degree of methylation comparable to the MGly + AS reaction system, albeit with different location and structure.

This methylation, along with the aromatic and/or highly conjugated nature of many of these compounds, leads to chromophoric behavior that is red-shifted from that of the imidazoles, pyrazines, and oxazoles that are often observed in CVOC + nitrogen-containing compound reaction systems. While GAld itself has markedly lower MAC compared to other CVOCs, the oligomeric products generated upon reaction with MeAm result in enhanced chromophoricity. Aged solutions exhibit 5−10 times higher light absorbance in the 280 nm region compared to GAld + AS solutions and a secondary peak comparable in MAC to that of the MGly + AS system when aged for similar durations.[28] The heterocyclic, vinylogous amidines and iminium cations also affect the light absorbing properties of this system; these molecules tend to have absorption transitions at lower energies than their similar less-conjugated counterparts.

While ambient atmospheric concentrations of GAld and MeAm are relatively low, the contribution of this reaction system to light absorption above 300 nm indicates that more research is needed to understand reaction systems that exhibit red-shifted behavior compared to the previously studied CVOC + AS systems.[15,16,28] The chemistry presented in this work implies a departure from the simplistic assumption that similarly structured CVOC + nitrogen-containing compounds behave analogously to one another when only differing by a methylation,[5] as is observed when comparing Gly + AS and MGly + AS reaction systems.[26,43,44] While it has been observed that GAld will yield different branching ratios and somewhat different SOA products compared to Gly,[15] the methylation from MeAm compared to AS imparts further nuance to this reaction system and provides plausible pathways for SOA products that would otherwise not be possible from the predominant CVOCs present within ambient aqueous aerosols. The surface tension measurements further support this; as the overall degree of methylation that exists in the GAld + MeAm system is comparable to the MGly + AS system, the lack of notable shift in surface activity in aged solutions implies that the methylation of the CVOC component in this chemistry results in more dramatic physical changes from SOA chemistry compared to that of the nitrogen-containing element.

In addition, the profound differences in overall structure of larger (3+) oligomers in the GAld + MeAm system implies that the concurrent presence of MeAm and AS in CVOC aqueous aerosols can result in yet further diversity of SOA products than previously expected. Conversely, a wide range of observed aqueous SOA products in ambient aerosol could plausibly be explained by the presence of few precursor compounds, which have reacted in a variety of ways depending on the relative concentrations of nitrogen-containing reactants (e.g., ammonium vs methylamine).

■ ASSOCIATED CONTENT

Supporting Information

The Supporting Information is available free of charge at https://pubs.acs.org/doi/10.1021/acsearthspacechem.4c00200.

Selected ion monitoring chromatograms, structures, and fragmentation information for all identified products; calculated UV−visible absorption data for all identified products (PDF)

https://doi.org/10.1021/acsearthspacechem.4c00200
ACS Earth Space Chem. XXXX, XXX, XXX−XXX

AUTHOR INFORMATION

Corresponding Author

Melissa M. Galloway − *Department of Chemistry, Lafayette College, Easton, Pennsylvania 18042, United States;* orcid.org/0000-0002-8518-1888; Phone: (610)330-5206; Email: gallowam@lafayette.edu

Authors

Camille L. Carthy − *Department of Chemistry, Lafayette College, Easton, Pennsylvania 18042, United States;* Present Address: Albert Einstein College of Medicine, Bronx, New York 10461, United States

Erin O'Leary − *Department of Chemical and Biomolecular Engineering, Lafayette College, Easton, Pennsylvania 18042, United States*

Swetha Tadisina − *Department of Chemistry, Lafayette College, Easton, Pennsylvania 18042, United States*

Daniel R. Griffith − *Department of Chemistry, Lafayette College, Easton, Pennsylvania 18042, United States;* orcid.org/0000-0002-0361-8290

Heidi P. Hendrickson − *Department of Chemistry, Lafayette College, Easton, Pennsylvania 18042, United States;* orcid.org/0000-0002-5012-738X

Joseph L. Woo − *Department of Chemical and Biomolecular Engineering, Lafayette College, Easton, Pennsylvania 18042, United States;* orcid.org/0000-0001-7264-3425

Complete contact information is available at: https://pubs.acs.org/10.1021/acsearthspacechem.4c00200

Author Contributions

The manuscript was written through the contributions of all authors. All authors have given approval to the final version of the manuscript.

Funding

Funding for this work was provided by the National Science Foundation (MRI-1626100). Computational resources were provided in part by the MERCURY consortium (https://mercuryconsortium.org/) under NSF grants CHE-1229354, CHE-1662030, and CHE-2018427. E.O. project support has been generously provided by the Clare Boothe Luce Program for Women in STEM.

Notes

The authors declare no competing financial interest.

ACKNOWLEDGMENTS

Funding for this work was provided by the National Science Foundation (MRI-1626100). Computational resources were provided in part by the MERCURY consortium (https://mercuryconsortium.org/) under NSF grants CHE-1229354, CHE-1662030, and CHE-2018427. E.O. project support has been generously provided by the Clare Boothe Luce Program for Women in STEM.

REFERENCES

(1) Powelson, M. H.; Espelien, B.; Hawkins, L. N.; Galloway, M. M.; De Haan, D. O. Brown carbon formation by aqueous-phase carbonyl compound reactions with amines and ammonium sulfate. *Environ. Sci. Technol.* **2014**, *48* (2), 985−993.

(2) Laskin, A.; Laskin, J.; Nizkorodov, S. A. Chemistry of atmospheric brown carbon. *Chem. Rev.* **2015**, *115* (10), 4335−4382.

(3) Hahad, O.; Lelieveld, J.; Birklein, F.; Lieb, K.; Daiber, A.; Münzel, T. Ambient Air Pollution Increases the Risk of Cerebrovascular and Neuropsychiatric Disorders through Induction of Inflammation and Oxidative Stress. *International Journal of Molecular Sciences* **2020**, *21* (12), 4306.

(4) Marrero-Ortiz, W.; Hu, M.; Du, Z.; Ji, Y.; Wang, Y.; Guo, S.; Lin, Y.; Gomez-Hermandez, M.; Peng, J.; Li, Y.; et al. Formation and Optical Properties of Brown Carbon from Small α-Dicarbonyls and Amines. *Environ. Sci. Technol.* **2019**, *53* (1), 117−126.

(5) Sharp, J. R.; Grace, D. N.; Ma, S.; Woo, J. L.; Galloway, M. M. Competing Photochemical Effects in Aqueous Carbonyl/ Ammonium Brown Carbon Systems. *ACS Earth Space Chem.* **2021**, *5* (8), 1902−1915.

(6) Kampf, C. J.; Filippi, A.; Zuth, C.; Hoffmann, T.; Opatz, T. Secondary brown carbon formation via the dicarbonyl imine pathway: nitrogen heterocycle formation and synergistic effects. *Phys. Chem. Chem. Phys.* **2016**, *18* (27), 18353−18364.

(7) Galloway, M. M.; Huisman, A. J.; Yee, L. D.; Chan, A. W. H.; Loza, C. L.; Seinfeld, J. H.; Keutsch, F. N. Yields of oxidized volatile organic compounds during the OH radical initiated oxidation of isoprene, methyl vinyl ketone, and methacrolein under high-NO_x conditions. *Atmos. Chem. Phys.* **2011**, *11* (21), 10779−10790.

(8) Ortiz-Montalvo, D. L.; Lim, Y. B.; Perri, M. J.; Seitzinger, S. P.; Turpin, B. J. Volatility and Yield of Glycolaldehyde SOA Formed through Aqueous Photochemistry and Droplet Evaporation. *Aerosol Sci. Technol.* **2012**, *46* (9), 1002−1014.

(9) Yu, G.; Bayer, A. R.; Galloway, M. M.; Korshavn, K. J.; Fry, C. G.; Keutsch, F. N. Glyoxal in aqueous ammonium sulfate solutions: Products, kinetics and hydration effects. *Environ. Sci. Technol.* **2011**, *45* (15), 6336−6342.

(10) Perri, M. J.; Seitzinger, S.; Turpin, B. J. Secondary organic aerosol production from aqueous photooxidation of glycolaldehyde: Laboratory experiments. *Atmos. Environ.* **2009**, *43* (8), 1487−1497.

(11) Ge, X.; Wexler, A. S.; Clegg, S. L. Atmospheric amines − Part I. *A review. Atmos. Environ.* **2011**, *45* (3), 524−546.

(12) Yi, Y.; Zhou, X.; Xue, L.; Wang, W. Air pollution: formation of brown, lighting-absorbing, secondary organic aerosols by reaction of hydroxyacetone and methylamine. *Environ. Chem. Lett.* **2018**, *16* (3), 1083−1088.

(13) De Haan, D. O.; Tolbert, M. A.; Jimenez, J. L. Atmospheric condensed-phase reactions of glyoxal with methylamine. *Geophys. Res. Lett.* **2009**, *36* (11), L11819.

(14) Grace, D. N.; Lugos, E. N.; Ma, S.; Griffith, D. R.; Hendrickson, H. P.; Woo, J. L.; Galloway, M. M. Brown Carbon Formation Potential of the Biacetyl−Ammonium Sulfate Reaction System. *ACS Earth Space Chem.* **2020**, *4* (7), 1104−1113.

(15) Grace, D. N.; Sharp, J. R.; Holappa, R. E.; Lugos, E. N.; Sebold, M. B.; Griffith, D. R.; Hendrickson, H. P.; Galloway, M. M. Heterocyclic Product Formation in Aqueous Brown Carbon Systems. *ACS Earth Space Chem.* **2019**, *3* (11), 2472−2481.

(16) Lin, P.; Laskin, J.; Nizkorodov, S. A.; Laskin, A. Revealing Brown Carbon Chromophores Produced in Reactions of Methylglyoxal with Ammonium Sulfate. *Environ. Sci. Technol.* **2015**, *49* (24), 14257−14266.

(17) De Haan, D. O.; Tapavicza, E.; Riva, M.; Cui, T.; Surratt, J. D.; Smith, A. C.; Jordan, M.-C.; Nilakantan, S.; Almodovar, M.; Stewart, T. N.; et al. Nitrogen-Containing, Light-Absorbing Oligomers Produced in Aerosol Particles Exposed to Methylglyoxal, Photolysis, and Cloud Cycling. *Environ. Sci. Technol.* **2018**, *52* (7), 4061−4071.

(18) Hawkins, L. N.; Welsh, H. G.; Alexander, M. V. Evidence for pyrazine-based chromophores in cloud water mimics containing methylglyoxal and ammonium sulfate. *Atmos. Chem. Phys.* **2018**, *18* (16), 12413−12431.

(19) Yi, Y.; Cao, Z.; Zhou, X.; Xue, L.; Wang, W. Formation of aqueous-phase secondary organic aerosols from glycolaldehyde and ammonium sulfate/amines: A kinetic and mechanistic study. *Atmos. Environ.* **2018**, *181*, 117−125.

(20) Rodriguez, A. A.; Rafla, M. A.; Welsh, H. G.; Pennington, E. A.; Casar, J. R.; Hawkins, L. N.; Jimenez, N. G.; de Loera, A.; Stewart, D. R.; Rojas, A.; et al. Kinetics, Products, and Brown Carbon Formation by Aqueous-Phase Reactions of Glycolaldehyde with Atmospheric Amines and Ammonium Sulfate. *J. Phys. Chem. A* **2022**, *126*, 5375.

(21) De Haan, D. O.; Hawkins, L. N.; Welsh, H. G.; Pednekar, R.; Casar, J. R.; Pennington, E. A.; de Loera, A.; Jimenez, N. G.; Symons, M. A.; Zauscher, M.; et al. Brown Carbon Production in Ammonium- or Amine-Containing Aerosol Particles by Reactive Uptake of Methylglyoxal and Photolytic Cloud Cycling. *Environ. Sci. Technol.* **2017**, *51* (13), 7458−7466.
(22) De Haan, D. O.; Hawkins, L. N.; Kononenko, J. A.; Turley, J. J.; Corrigan, A. L.; Tolbert, M. A.; Jimenez, J. L. Formation of Nitrogen-Containing Oligomers by Methylglyoxal and Amines in Simulated Evaporating Cloud Droplets. *Environ. Sci. Technol.* **2011**, *45* (3), 984−991.
(23) De Haan, D. O.; Pajunoja, A.; Hawkins, L. N.; Welsh, H. G.; Jimenez, N. G.; De Loera, A.; Zauscher, M.; Andretta, A. D.; Joyce, B. W.; De Haan, A. C.; et al. Methylamine's Effects on Methylglyoxal-Containing Aerosol: Chemical, Physical, and Optical Changes. *ACS Earth Space Chem.* **2019**, *3* (9), 1706−1716.
(24) Beier, T.; Cotter, E. R.; Galloway, M. M.; Woo, J. L. In Situ Surface Tension Measurements of Hanging Droplet Methylglyoxal/Ammonium Sulfate Aerosol Mimics under Photooxidative Conditions. *ACS Earth Space Chem.* **2019**, *3* (7), 1208−1215.
(25) Sareen, N.; Schwier, A. N.; Lathem, T. L.; Nenes, A.; McNeill, V. F. Surfactants from the gas phase may promote cloud droplet formation. *Proc. Natl. Acad. Sci. U.S.A* **2013**, *110* (8), 2723−2728.
(26) Sareen, N.; Schwier, A. N.; Shapiro, E. L.; Mitroo, D.; McNeill, V. F. Secondary organic material formed by methylglyoxal in aqueous aerosol mimics. *Atmos. Chem. Phys.* **2010**, *10* (3), 997−1016.
(27) Grace, D. N.; Sebold, M. B.; Galloway, M. M. Separation and detection of aqueous atmospheric aerosol mimics using supercritical fluid chromatography−mass spectrometry. *Atmos. Meas. Technol.* **2019**, *12* (7), 3841−3851.
(28) Fan, M.; Ma, S.; Ferdousi, N.; Dai, Z.; Woo, J. L. Modeling of Carbonyl/Ammonium Sulfate Aqueous Brown Carbon Chemistry via UV/Vis Spectral Decomposition. *Atmosphere* **2020**, *11* (4), 358.
(29) *Gaussian*; Gaussian, Inc.: Wallingford, CT, 2016.
(30) Chai, J.-D.; Head-Gordon, M. Long-range corrected hybrid density functionals with damped atom−atom dispersion corrections. *Phys. Chem. Chem. Phys.* **2008**, *10* (44), 6615−6620.
(31) Grimme, S. Semiempirical GGA-type density functional constructed with a long-range dispersion correction. *J. Comput. Chem.* **2006**, *27* (15), 1787−1799.
(32) Krishnan, R.; Binkley, J. S.; Seeger, R.; Pople, J. A. Self-consistent molecular orbital methods. XX. A basis set for correlated wave functions. *J. Chem. Phys.* **1980**, *72* (1), 650−654.
(33) McLean, A. D.; Chandler, G. S. Contracted Gaussian basis sets for molecular calculations. I. Second row atoms, Z = 11−18. *J. Chem. Phys.* **1980**, *72* (10), 5639−5648.
(34) Barone, V.; Cossi, M. Quantum Calculation of Molecular Energies and Energy Gradients in Solution by a Conductor Solvent Model. *J. Phys. Chem. A* **1998**, *102* (11), 1995−2001.
(35) Cossi, M.; Rega, N.; Scalmani, G.; Barone, V. Polarizable dielectric model of solvation with inclusion of charge penetration effects. *J. Chem. Phys.* **2001**, *114* (13), 5691−5701.
(36) Martin, R. L. Natural transition orbitals. *J. Chem. Phys.* **2003**, *118* (11), 4775−4777.
(37) *iQmol*. 2020. http://iqmol.org/index.html.
(38) *Gaussview*; Semichem Inc.: Shawnee Mission, KS, 2016.
(39) Kua, J.; Galloway, M. M.; Millage, K. D.; Avila, J. E.; De Haan, D. O. Glycolaldehyde Monomer and Oligomer Equilibria in Aqueous Solution: Comparing Computational Chemistry and NMR Data. *J. Phys. Chem. A* **2013**, *117* (14), 2997−3008.
(40) Kampf, C. J.; Jakob, R.; Hoffmann, T. Identification and characterization of aging products in the glyoxal/ammonium sulfate system – implications for light-absorbing material in atmospheric aerosols. *Atmos. Chem. Phys.* **2012**, *12* (14), 6323−6333.
(41) Nozière, B.; Córdova, A. A Kinetic and Mechanistic Study of the Amino Acid Catalyzed Aldol Condensation of Acetaldehyde in Aqueous and Salt Solutions. *J. Phys. Chem. A* **2008**, *112* (13), 2827−2837.
(42) Ackendorf, J. M.; Ippolito, M. G.; Galloway, M. M. pH Dependence of the Imidazole-2-carboxaldehyde Hydration Equilibrium: Implications for Atmospheric Light Absorbance. *Environ. Sci. Technol. Lett.* **2017**, *4* (12), 551−555.
(43) Schwier, A. N.; Sareen, N.; Mitroo, D.; Shapiro, E. L.; McNeill, V. F. Glyoxal-Methylglyoxal Cross-Reactions in Secondary Organic Aerosol Formation. *Environ. Sci. Technol.* **2010**, *44* (16), 6174−6182.
(44) Shapiro, E. L.; Szprengiel, J.; Sareen, N.; Jen, C. N.; Giordano, M. R.; McNeill, V. F. Light-absorbing secondary organic material formed by glyoxal in aqueous aerosol mimics. *Atmos. Chem. Phys.* **2009**, *9* (7), 2289−2300.

https://doi.org/10.1021/acsearthspacechem.4c00200
ACS Earth Space Chem. XXXX, XXX, XXX−XXX